Narrow band resonant grating of 100% reflection under normal incidence

Nathalie Destouches, J.C. Pommier, O. Parriaux, T. Clausnitzer, N. Lyndin, S. Tonchev

Narrow band resonant grating of 100% reflection under normal incidence

N. Destouches, J.-C. Pommier, and O. Parriaux

Laboratoire Hubert Curien UMR 5516 (formerly LTSI)
Université Jean Monnet 18 Rue Benoît Lauras F-42000 Saint-Etienne,
parriaux@univ-st-etienne.fr

T. Clausnitzer

Institut für Angewandte Physik, Friedrich-Schiller Universität, Max-Wien Platz 1, 07743 Jena, Germany

N. Lyndin

Institute of General Physics, Vavilova 38, 117942 Moscow, Russian Federation

S. Tonchev

On leave from the Institute of Solid State Physics, Sofia, Bulgaria

Abstract: A resonant grating mirror comprising a multilayer submirror and a grating slab waveguide submirror exhibiting constructive mutual reflection is shown experimentally to provide zero transmission. Its reflection line width of less than 1 nm, its polarization selectivity and low overall loss make the device usable as a longitudinal mode filter in a disk laser in the 1000-1100 nm wavelength range.

OCIS codes: (050.2770) Gratings; (310.2790) Guided waves; (140.3570) Single-mode lasers; (230.4000) Microstructure fabrication; (310.6860) Thin films, optical properties; (050.1930) Dichroism.

References and links

1. F. Pigeon, O. Parriaux, Y. Ouerdane, and A. V. Tishchenko, "Polarizing grating mirror for CW Nd:YAG microchip lasers," IEEE Photon.Technol. Lett. **12**, 648-650 (2000).
2. O. Parriaux, A. V. Tishchenko, and F. Pigeon, "Associating a lossless polarizing function in multilayer laser mirrors by means of a resonant grating," Photonics Europe Proc. SPIE Vol. **6187**, 61870B (Apr. 25, 2006).
3. J.-F. Bisson, O. Parriaux, J. C. Pommier, S. Tonchev and K. Ueda, "A polarization-stabilized microchip laser using a resonant grating mirror," Appl. Phys. B to be published
4. E. Gamet, J. C. Pommier, S. Reynaud, S. Tonchev, O. Parriaux, J.-F. Bisson, K. I. Ueda, and T. Ito, "Polarizing multilayer laser mirror using constructive zeroth order resonant grating reflexion," Diffractive Optics abstracts pp 157-158, Warsaw, Poland (3-7 Sept. 2005)
5. T. Moser, M. A. Ahmed, F. Pigeon, O. Parriaux, E. Wyss, and Th. Graf, "Generation of radially polarized beams in Nd : YAG lasers with polarization selective mirrors," Laser Phys. Lett. **1**, 234-236 (2004).
6. L Li and J Hirsh, "All-dielectric high-efficiency reflection gratings made with multilayer thin-film coatings," Opt. Lett. **20**, 1349-1351 (1995).
7. T. Clausnitzer, E.-B. Kley, A. Tünnermann, A. Bunkowski, O. Burmeister, K. Danzmann, R. Schnabel, S. Gliech, and A. Duparré, "Ultra low-loss low-efficiency diffraction gratings," Opt. Express **13**, 4370-4378 (2005).
8. G. A. Golubenko, A. S. Svakhin, A. V. Tishchenko, and V. A Sychugov, "Total reflection of light from the corrugated surface of a dielectric waveguide," Sov. J. Quantum Electron. **15**, 886-887 (1985)
9. I. A. Avrutsky and V. A. Sychugov, "Reflection of a beam of finite size from a corrugated waveguide," J. Mod. Opt. **36**, 1527 (1989)
10. E. Bonnet, X. Letartre, A. Cachard, A. V. Tishchenko and O. Parriaux, "High resonant reflection of a confined free space beam by a high contrast segmented waveguide," Opt. Quantum Electron. **35**, 1025-1036 (2003).
11. F. Lemarchand, A. Sentenac, E. Cambril and H. Giovannini, "Study of the resonant behaviour of waveguide gratings: increasing the angular tolerance of guided-mode filters," J. Opt. A: Pure Appl. Opt. **1,** 545-551 (1999).

#76035 - $15.00 USD Received 13 October 2006; revised 7 November 2006; accepted 7 November 2006

12. A. V. Tishchenko and N. Lyndin, "The true modal method solves intractable problems: TM incidence on fine metal slits (but the C method also !)," Workshop on grating theory, Clermont-Ferrand, France (June 2004)
13. S. Schlichtherle, G. N. Strauss, H. Tafelmaier, D. Huber, and H. K. Pulker, "Reactive ion voltage ion plating," Vakuum in forschung und praxis **17**, 210-217 (2005).
14. I. A. Avrutsky, G. A. Golubenko, V. A. Sychugov, and A. V. Tishchenko, "Spectral and laser characteristics of a mirror with a corrugated waveguide on its surface," Sov. J. Quantum Electron. **16**, 1063 (1986).
15. F. R. Flory, *Thin films for optical systems* (Marcel Dekker, 1995).

1. Introduction

Resonant grating mirrors based on the excitation under normal incidence of a guided mode of a high index layer (or set of layers) belonging to a multilayer mirror have been shown to induce into said multilayer mirror a dichroic character [1]. This resonant effect was used in multilayer laser mirrors to monolithically control the polarization of the emission [2]. The direction of linear polarization is controlled by means of a rectilinear grating [3- 4] whereas a circular grating permits the generation of the very much wanted radially polarized mode as shown in a high power Nd:YAG laser [5]. The polarizing mechanism in a resonant grating mirror is based on the association of a standard multilayer reflector achieving most of the reflection and a pair of corrugated high and low index layers exhibiting so-called abnormal or resonant reflection thanks to the excitation by the incident beam of a guided mode of the high index layer via the grating. The reflection spectrum is thus composed of a wide band reflection pedestal produced by the multilayer and a reflection peak on top of the latter at the waveguide resonance. Whether the signature of the resonance is a peak or a dip in the reflection pedestal depends on the thickness of the low index buffer layer separating the multilayer and waveguide grating submirrors, i.e., depends whether the interference between the fields reflected by the two submirrors is constructive or destructive. Both options can be used for polarizing a laser beam: if the interference is constructive (there is a peak in the reflection spectrum), it is the coupled polarization which experiences the higher reflection coefficient and will therefore lase [3, 4] whereas in case of destructive interference, the non-coupled polarization will lase [1]. Both cases have been demonstrated experimentally. For the polarizing device to operate properly, the resonance must take place with normal excitation in the gain bandwidth of the active laser material; this imposes the following condition between the central wavelength λ of the gain bandwidth and the grating period Λ: $\Lambda = \lambda/n_e$ where n_e is the effective index of the coupled mode at wavelength λ. This is not too easy to achieve without post-fabrication trimming because today's multilayer technologies do not exhibit sufficient reproducibility on the layer index and thickness: multilayer technologies can usually reproduce an optical path, but not the index and thickness separately. Therefore the effective index is not a priori known with sufficient accuracy. This is still a subject of concern for the development of resonant gratings applications. It is therefore still the task of the structure designer to give sufficient tolerances on the position of the resonance condition. A broadening of the resonance is the most obvious solution; this also what is required at any rate in a polarizing mirror since it is the whole gain bandwidth which must exhibit the dichroism effect.

The present paper reports on a different application of a resonant mirror to the control of laser emission. The objective is here to achieve very close to 100% resonant reflection under normal incidence and the narrowest possible reflection peak in order to select a single or narrow group of longitudinal laser modes. Such function is needed in interferometry and for second harmonic generation for instance. It is the same type of resonant mirror which will be used as described above for polarization control. However, the very specifications placed on the mirror will permit to learn more on the characteristics and limits of such resonant diffractive elements.

The present mirror is intended to be the rear mirror of an extended cavity semiconductor disk laser.

#76035 - $15.00 USD Received 13 October 2006; revised 7 November 2006; accepted 7 November 2006

2. Operation principle of a narrow band resonant laser mirror.

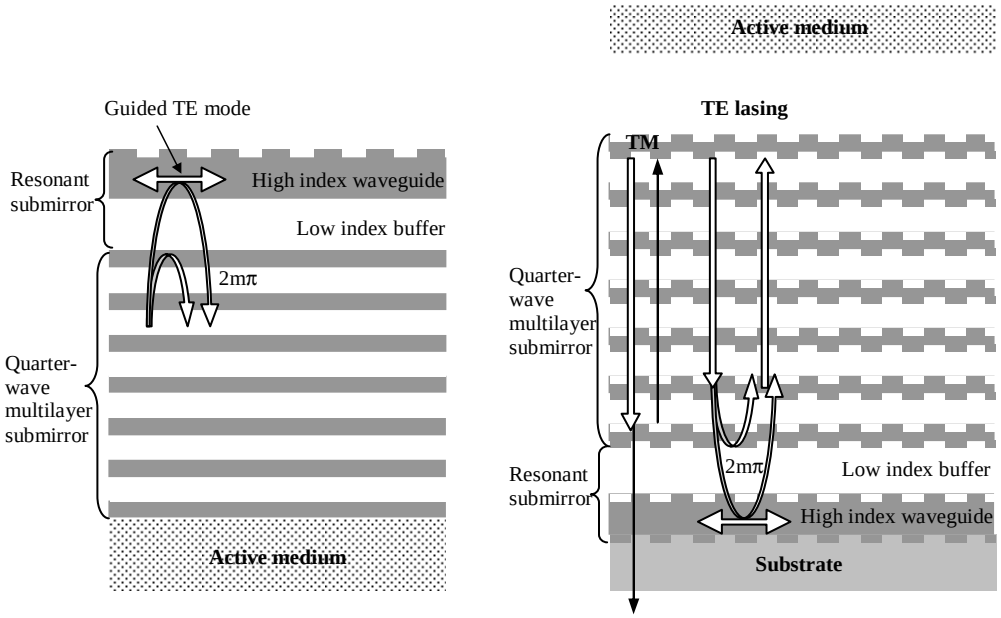

Fig. 1. (a). Operation principle of a polarizing mirror integrated to the active medium [4] (b) Operation principle of the narrow band resonant grating of the present study. In both structures light experiences constructive interference between multilayer and resonant mirrors.

The principle is the same as in the polarization filtering resonant mirror exhibiting constructive interference between the broad band ground reflection provided by a multilayer submirror and that provided by the waveguide resonance [3, 4]. Figure 1(a) is the sketch of the corresponding resonant mirror. The mirror in the present application is however the rear mirror of an extended cavity laser which must exhibit the least possible loss. Resonant reflection from a waveguide grating is known not to provide 100% reflection although it is theoretically possible: the scattering losses due to imperfect corrugation and waveguide absorption losses limit the practically achievable reflection coefficient to about 98%. As a consequence, the reflection threshold provided by the very low loss multilayer submirror must be as high as possible, leaving only a few percents of reflection to the highly selective resonant submirror, the only concern being that the spectral components outside the reflection peak do not lase. At this point it is worth mentioning that the narrow spectral filtering of the present device is inherently associated with polarization filtering: only that polarization which is coupled will experience amplification since its reflection is larger than that of the uncoupled polarization. Another specificity of the present mirror is that it is not integrated to the active medium unlike in the microchip laser demonstration in Ref. [3]. It is a stand alone mirror. The rear mirror should be looking at the inside of the laser cavity, its substrate being outside the cavity. If the mirror is fabricated according to the usual sequence of processes, the multilayer is deposited first with the two or three layers which will become the resonant submirror once the corrugation of the last high index layer has been fabricated. This is however not a desirable solution since it would imply that the wave impinging onto the rear mirror would first “see” the resonant submirror, then the multilayer. As a result, most of the reflection would be produced by the resonant mechanism with its losses of a few percents. Consequently, the resonant submirror must be located past the multilayer submirror on the way of the incident wave. This imposes the somewhat unusual configuration as sketched in

#76035 - $15.00 USD Received 13 October 2006; revised 7 November 2006; accepted 7 November 2006

Fig. 1(b) where the mirror substrate gets first corrugated, then the resonant submirror layers are deposited as well as the layers of the multilayer submirror at once in the said order. The fact that all layers or part of them only are corrugated has often been a concern: it was once shown that such characteristics leads to a strong perturbation of the optical function [6], more recently, the same feature was shown to lead to a reduction of the scattering [7]. It is important to point out that we are making use here of a resonant diffraction mechanism where the field in the waveguide is so large that a very shallow corrugation of hardly 15 nm is sufficient to provoke a major effect. Considering that the period is of the order of 500-600 nm, the corrugation aspect ratio is very small and unlikely to lead to adverse consequences on the operation of the multilayer submirror. This is what the experimental results will confirm indeed. It must also be said that the layer deposition technology is that of ion plating which ensures a conformal reproduction of the corrugation amplitude up to a large number of layers. The AFM scan of the last layer of the present 21 layers multilayer, 2.706 µm thick, made of alternate SiO_2 / Ta_2O_5 shows in Fig. 2(a) that there is a high degree of conformity with the scan made just after the etching of the fused quartz substrate [Fig. 2(b)]. Amazingly, ion plating even leads to an increase of the grating depth, in the present case from 17 nm to 23 nm. The period profile experiences a rounding of the ridges as if the first Fourier harmonics remained constant from the bottom silica corrugation to the last layer corrugation. A further technological and material study will undertake the analysis of this remarkable feature. This has the consequence that with such technology the behavior of all parts of the system can be modelised predicatively.

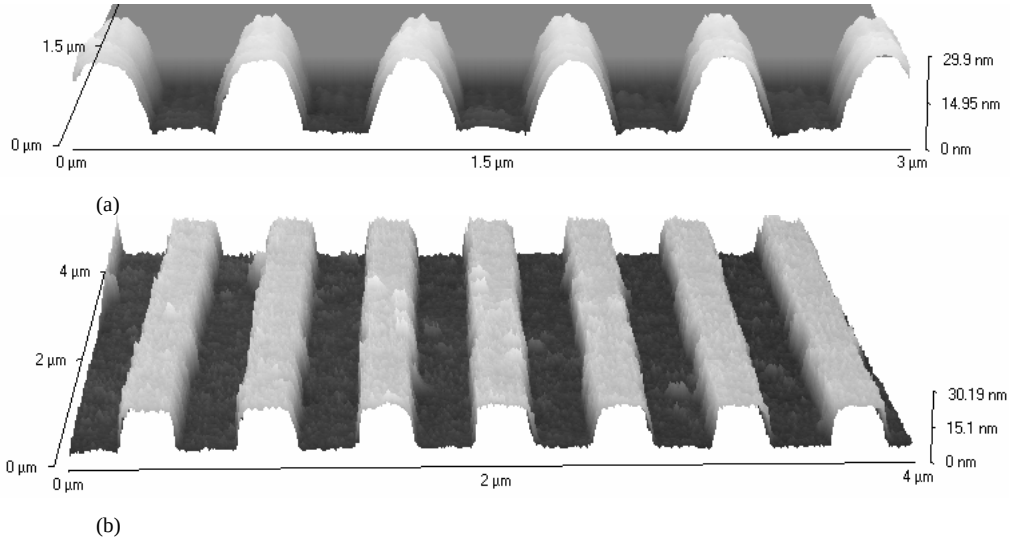

Fig. 2. AFM scan of the last Ta_2O_5 layer of the multilayer (a) and of the etched SiO_2 substrate (b). The grating depth in the last Ta_2O_5 layer is 23 nm whereas it is 17 nm on the substrate.

The most important element in the multilayer system is the grating waveguide placed on top of the corrugated substrate. The whole synthesis of this element is made on the basis of the physical understanding of waveguide grating resonances first developed by Sychugov and team in the mid eighties [8]. The grating waveguide is well isolated from the multilayer by the thick low index buffer layer. It is symmetrical (double corrugation and cover and substrate index nearly identical). In addition, as given in Table 1, the waveguiding layer with its 240 nm thickness of Ta_2O_5 of 2.18 index is very close to a half wave layer. This implies that the modulus of resonant reflection shows as a single peak with zero offset and no side dip; as a consequence, the resonant reflection can be simply placed as a quasi symmetrical peak on top of the multilayer ground reflection. Figure 3 shows that the transmission dip of the sole high

#76035 - $15.00 USD Received 13 October 2006; revised 7 November 2006; accepted 7 November 2006

index corrugated waveguiding layer surrounded by SiO_2 at both sides in the described conditions is symmetrical. The transmission falls from quasi 100% to zero as expected. The grating has a 559 nm period and a 21.6 nm deep sinusoidal corrugation. The transmission of the complete multilayer structure is represented by the dotted line; it confirms that the two submirror reflections superpose.

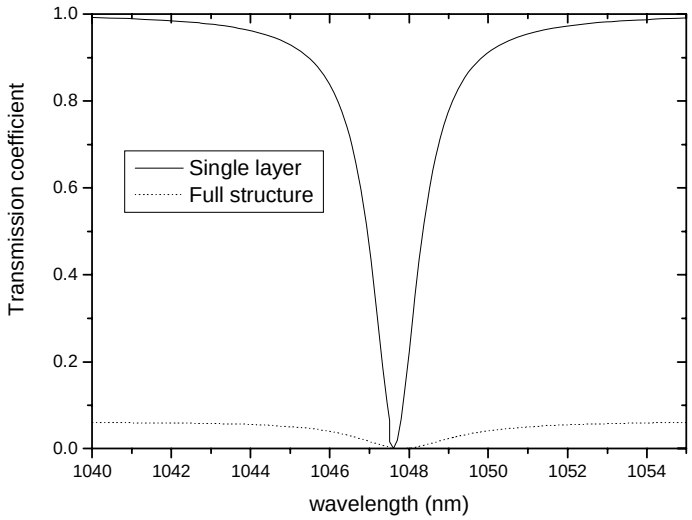

Fig. 3. Calculated transmission coefficient of the complete resonant mirror (doted line) and of the sole waveguide submirror (full line) versus wavelength in the resonance neighborhood.

The strength of the grating is such that there is 100% resonant reflection for an incident wave of imposed beam width. 400 nm beam width was imposed at the nominal wavelength of 1050 nm. How to dimension the grating strength for obtaining 100% resonant reflection for a beam of prescribed diameter is not a simple problem in the case of normal incidence. The phenomenological approach of resonant reflection teaches that the condition for 100% reflection in collinear incidence is $\alpha w > 2\pi$ where α is the radiation coefficient and w the width of the trace of a Gaussian incident beam on the waveguide grating plane [9]. This condition expresses the requirement that the excited guided wave does not propagate outside the impact zone of the incident beam so that the field overlap in the destructive interference between the 0^{th} order transmitted beam and the trapped then extracted beam in the transmission medium is close to 100%. Under normal incidence there is presently no simple expression between phenomenological parameters accounting for the coupling phenomena involved which are the + and -1^{st} orders waveguide coupling and the + and -2^{nd} orders intra-guide Bragg reflection. As underlined in previous works, this 2^{nd} order intraguide coupling may play a very important role [10, 11]. The strength which the resonant grating must have to give rise to 100% reflection of a beam of finite width is therefore calculated numerically in the normal incidence case; as all layer interfaces are essentially undulated, the C-method is ideally suited [12]. The relevant information which a plane wave numerical simulation can provide for the determination of the grating strength leading to 100% reflection of a beam of finite width w is to be found in the angular spectrum of the plane wave reflection around normal incidence. The full angular width $\Delta\theta_i$ of the angular spectrum is related with the propagation length of the coupled wave in the corrugated waveguide indeed, i.e., to the width w of the beam which can be efficiently reflected. For instance, if the beam is Gaussian, the angular width of the waveguide resonance which must be provided by the waveguide grating

#76035 - $15.00 USD Received 13 October 2006; revised 7 November 2006; accepted 7 November 2006

is: $\Delta\theta_i = \frac{4}{\pi}\frac{\lambda}{w}$, where λ is the wavelength in the considered material, air in the present laser case. As from here, the designer will use any grating code, for instance [12], to find out the grating depth, possibly the duty cycle [11] leading to 100% reflection of angular width $\Delta\theta_i$. It is this method which led to the design of the grating of Fig. 1(b) with sinusoidal groove depth of 20 nm.

The optimized multilayer is made of alternate SiO_2 and Ta_2O_5 layers. The refractive indices are those obtained by ion plating at 1050 nm wavelength, i.e., 1.48 and 2.18 respectively. The grating period is 560 nm, the rectangular grating depth 15.6 nm only and the line/space ratio is 1/1. The modelling made by means of the C-method of a sinusoidal corrugation concluded to a 20 nm depth peak to trough. At so shallow a grating depth the same grating strength is provided by binary and sinusoidal gratings in the ratio $\pi/4$ between the first harmonic of their development in series. Figure 4 is the optimised reflection spectrum of the TE polarization, assuming plane wave incidence and infinite grating length. The spectrum extends to the green region because the mirror has the additional function of reflecting the second harmonics as well, but this is not a point discussed in the present paper. The multilayer comprises at the cavity side a set of thinner low and high index layers: this is the quarter wave submirror stack for the generated second harmonics. The expected resonance width in the chosen configuration is 2.5 nm.

The IR multilayer stack shows clearly that the first high index layer at the substrate side is thicker than a quarter wave layer: this is the waveguide followed by the low index buffer of width w_b. The reflection coefficient of the sole corrugated waveguide layer in the absence of the multilayer with silica cover and substrate under normal incidence from the silica cover is found to be 100% in modulus with a phase of –179.7 degrees by means of the C method with a 20 nm deep sinusoidal grating, and 170° with the modal method and a 15.6 nm deep grating

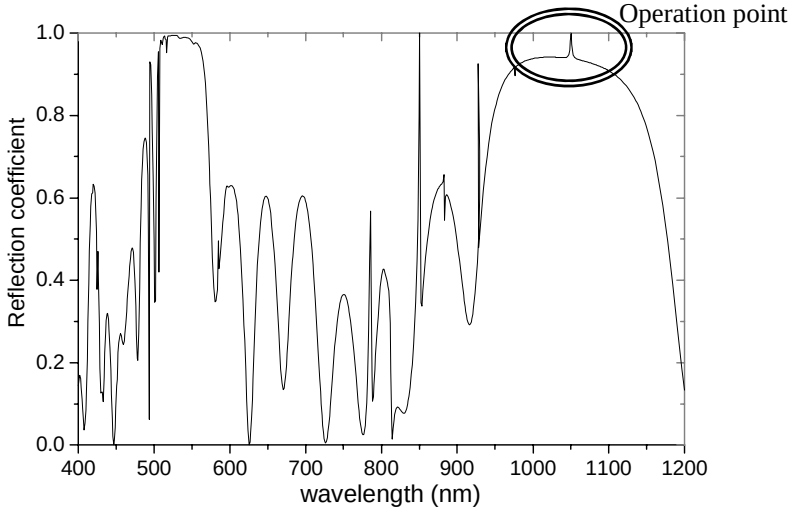

Fig. 4. Reflection coefficient of the optimised structure versus wavelength in the visible and IR regions with a peak at 1050 nm.

[12]. This confirms by the way that the resonant reflection phase is essentially π. With a low index buffer thickness of 561 nm one checks that the phase difference between the reflection from the multilayer and the resonant reflection at the resonance wavelength of 1050 nm at the interface between the last high index layer of the multilayer and the buffer is close to 390 degrees which confirms that the two reflection contributions add up essentially constructively. That the phase difference between the multilayer and resonant submirrors is not exactly 360°

#76035 - $15.00 USD Received 13 October 2006; revised 7 November 2006; accepted 7 November 2006

in the optimally designed structure does not question the relevance and general validity of the present physical representation: the interference is not exactly between two independent fields; the TE_0 waveguide mode field is well concentrated in the bottom high index layer indeed, however, as shown in Fig. 5, the buffer layer isolation is not complete and the modal field weakly extends its tail all through the multilayer.

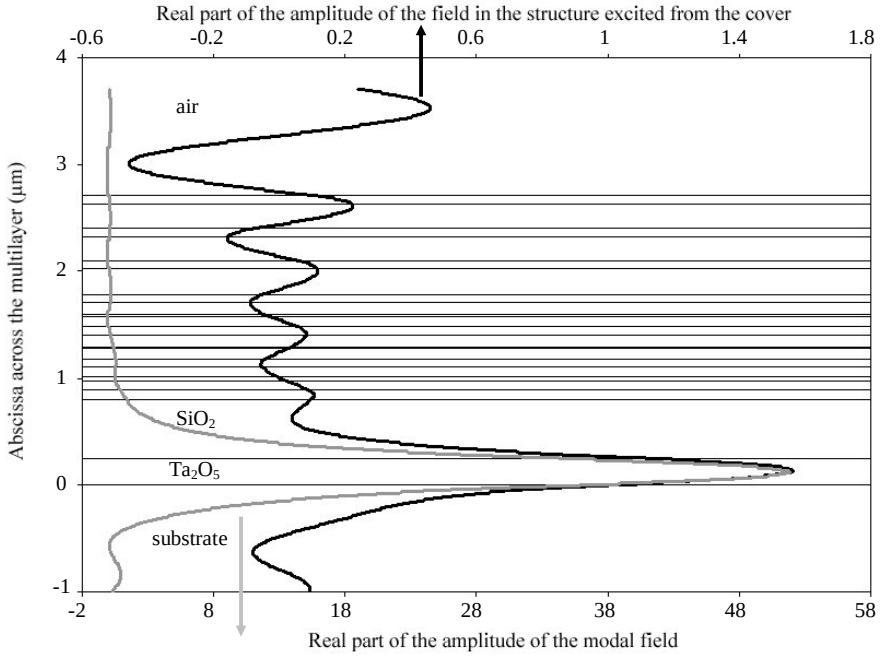

Fig. 5. Transverse electric field profile in the multilayer. Grey curve: TE_0 modal field, Black curve: field profile upon excitation from the air side. The horizontal lines show the different layers of the stack.

3. Experiment

The grating corrugation in the fused quartz substrate is obtained by first exposing a 300 nm thick positive resist to an interferogramme at the HeCd laser wavelength of 442 nm, then by reactive ion beam etching into the silica surface. Figure 2(b) is the AFM scan of the obtained binary grating of 559.1 nm period and 17 nm depth.

The multilayer is then deposited by ion plating [13]. The AFM scan of the surface after the deposition of the 2706 nm thick multilayer is also essentially binary with a depth of 23 nm, as shown in Fig. 2(a).

Figure 6 is a preliminary spectral measurement of the TE polarized transmission of the complete structure around 1050 nm wavelength. It reveals under normal incidence a sharp and deep dip on a wide band transmission background. The latter exhibits a periodic noise (with a period of about 0.3 nm) which actually is the signature of the Fabry-Pérot effect between the mirror and the back face of the fused quartz substrate. The different curves correspond to slightly different incidence angles. The amplitude of the interference noise is essentially the same for all curves. Non-normal incidence naturally exhibits a pair of transmission dips corresponding to forward and backward mode excitation placed symmetrically relatively to the central wavelength. These dips have a line width of about half that of normal incidence as expected from Ref. [14]. The spectral spacing between the two dips of a pair increases with the incidence angle. The measurements were made by using an optical fibre white light supercontinuum and a spectrometer of the type ANDO AQ-6315A Optical Spectrum analyzer

#76035 - $15.00 USD Received 13 October 2006; revised 7 November 2006; accepted 7 November 2006

ensuring a spectral resolution of 0.1 nm. The high spatial coherence of the source permits the separation between the angular and spectral effects. The beam diameter is about 1 mm. Index matching a prism at the backside of the grating substrate with glycerol (insert of Fig. 7), whose refractive index matches that of the silica substrate, reduces the oscillations due to the backside reflection and the resulting interference. This leads to the spectacular transmission spectra of Fig. 7 revealing that the TE line width is as small as 2.2 nm and that the transmission is practically cancelled. The transmission at resonance is two orders of magnitude below the off-resonance transmission. It is at the detection limit of the detector. Remarkable is the fact that the resonance wavelength is only 1 nm away from the expected nominal resonance wavelength taking into account the experimental values of the grating period and depth in the calculations. This is a result of the good control which ion plating ensures on the layer index and thickness. The experimental transmission curve exhibits a double dip which infers that the incidence is not exactly normal. Experimentally, the auto collimation reference is defined at a resolution better than 0.02 degree. This is confirmed by calculating the theoretical transmission coefficient of the structure if illuminated under an incidence angle of 0.015°: the resulting spectrum (dashed curve in Fig. 7) exhibits the same feature as the experimental curve with exactly the same 0.6 nm distance between the two dips. The line width under oblique incidence is proportional to the radiation coefficient α of the grating waveguide; in other words it scales as the square of the grating depth for small depths. Assuming for instance that the resonant reflection condition is satisfied for a beam of 400 μm diameter and a grating depth of 20 nm leading to a line width of 2 nm, the needed radiation coefficient for the resonant reflection of a 200 μm wide beam is doubled which is achieved by a grating of $\sqrt{2}$ larger grooves; this leads to a line width twice as wide: 4 nm. However, under normal incidence, the resonance situation is fundamentally different because two contra directional coupled modes are involved with second order coupling between them. The scaling rules between the line width and the grating parameters in the form of phenomenological parameters do not exist to our knowledge. Numerical modeling only can predict what line width is provided by a given resonant structure.

Figures 6 and 7 refer to transmission measurements. Nothing presently tells that zero transmission amounts to exactly 100% reflection at resonance. Reflection measurements are very difficult to make at high precision. Laser measurements may give a quantitative estimate of the losses due to grating scattering and waveguide absorption losses. This will be the subject of further experimental studies.

4. The loss issue

The present resonant reflection device exhibits remarkable characteristics: narrow line width and a hardly measurable transmission. That the transmission is zero at resonance doesn't mean that the reflection is 100% because the corrugation at all interfaces gives rise to scattering and furthermore the field trapping in the guided mode causes reinforced scattering at the waveguide corrugated boundaries. In addition, the field which gives rise to the reflection peak experiences waveguide absorption losses along the propagation length which in the present case of 100% resonant reflection of a 400 μm diameter beam is roughly 50 μm. These losses represent the limits of the present device. More generally, they represent the limits for the applicability of resonant gratings. From the absorption loss figures published in the literature [15] on vacuum deposited high index metal oxide films, it can be assumed that

#76035 - $15.00 USD Received 13 October 2006; revised 7 November 2006; accepted 7 November 2006

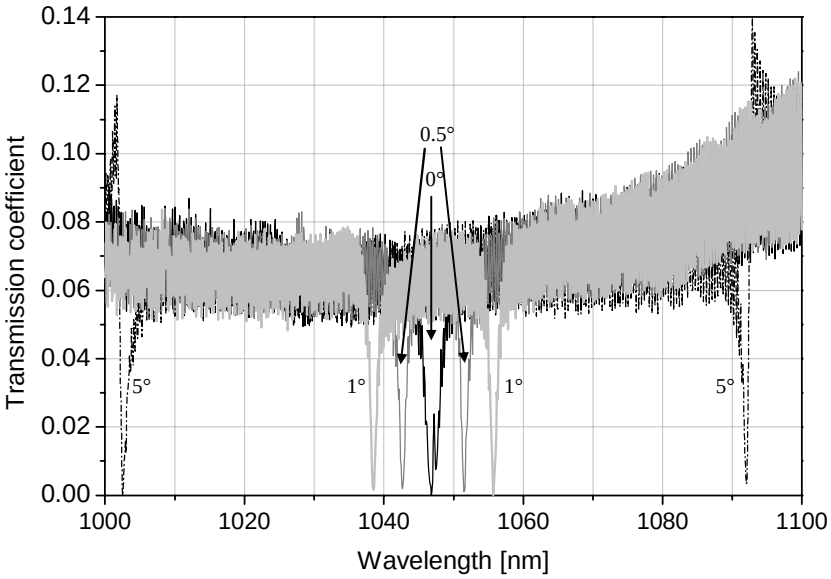

Fig. 6. Measured transmission spectra in TE polarization with the incidence angle as a parameter showing the normal incidence central dip at 1047 nm wavelength and three symmetrical pairs of dips.

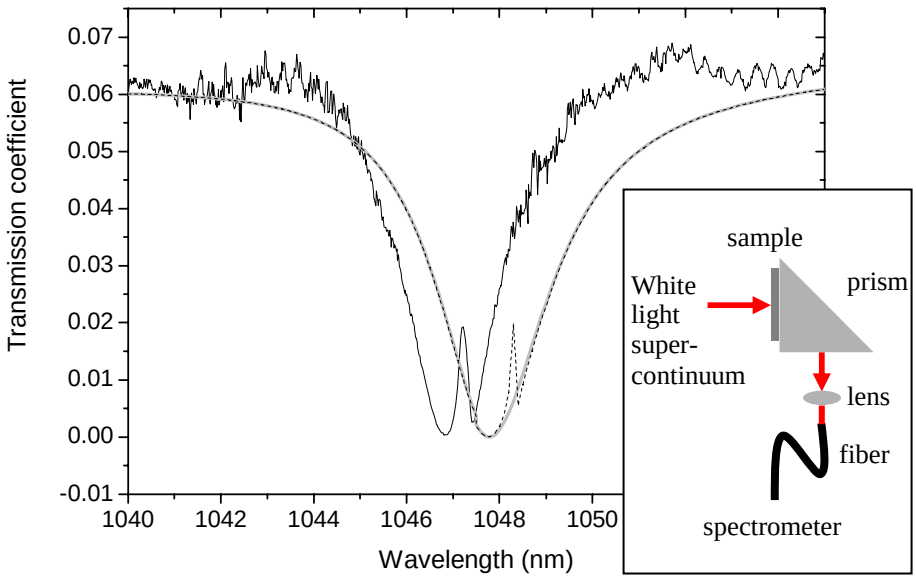

Fig. 7. Transmission coefficient of the structure around 1050 nm after suppression of backside reflection (insert). The grey curve is the theoretical transmission coefficient taking into account the measured grating parameters (period of 559.1 nm and depth of 17 nm) and the layers thicknesses of table 1 under normal incidence. The dashed curve is the theoretical spectrum obtained under an incidence angle of 0.015°

#76035 - $15.00 USD Received 13 October 2006; revised 7 November 2006; accepted 7 November 2006

0.1 dB/100 µm is achievable; as such loss affects the resonant part of the reflected power (less than 10%), absorption losses as small as 0.1% must be within reach. Therefore, the most limiting factor may be the scattering level.

The issue of scattering measurement under the condition of narrow line resonant reflection is a specific metrology problem requiring a very high spectral and angular resolution to retrieve the sole characteristics of resonant scattering. Early results have led to an adapted methodology which is under development.

5. Conclusion

The present paper reports on the demonstration of a further optical function that a resonant grating can perform for laser control : line narrowing leading to longitudinal mode filtering. It is demonstrated that the constructive association between a broadband multilayer and a waveguide grating permits to fully benefit from the narrow filtering property of waveguide grating resonant reflection without the penalty of its absorption and scattering losses. The design of the resonant mirror is made via an intelligible synthesis process based on field diffraction and interference, only the optimisation step being left to numerical modelling. This paper provides the methodology enabling the design of a wide variety of similar devices operating at different wavelengths and/or made of different materials.

A line as narrow as 2 nm is obtained at 1050 nm wavelength for a beam of 400 nm diameter by an embedded binary grating of 15 nm depth. A remarkable feature is the achievement of practically zero transmission at resonance by means of a multilayer structure having all interfaces corrugated. Although the precise measurement of the resulting scattering and absorption losses still has to be made, the present results already show that reversing the layer order in a resonant structure is possible without detrimental consequence. This is true for ion plating deposition technology characterized by a high conformity between interface corrugations. Whether the same is more generally true with other deposition technologies can not be stated; it is probable that it is, since the corrugation is very shallow on the one hand, and the layer responsible for the resonance is the first one deposited on the corrugated substrate on the other hand. A further feature in favour of ion plating is the reproducibility of the layer index and thickness allowing the resonance to be predicted within 0.2 %.

Further investigations are in process with the present mirror in a laser cavity for a finer evaluation of the spectral narrowing effect, of the polarization properties and of flux resistance as well as on the general scattering characteristics of this resonant corrugated multilayer.

Acknowledgment

The authors are grateful to the Institute of Applied Physics of Friedrich-Schiller-University Jena for making their high resolution spectral measurement set-up available. They also thank Dr. A. Duparré, Fraunhofer IOF Jena, for her contribution in the analysis of the scattering issue under grating coupled resonance.

This work is part of an initiative on resonant gratings within the European network of excellence on microoptics NEMO.

#76035 - $15.00 USD Received 13 October 2006; revised 7 November 2006; accepted 7 November 2006